# Quantum Electrodynamics and Quantum Optics: Lecture 5

Fall 2025

# Hong-Ou-Mandel effect

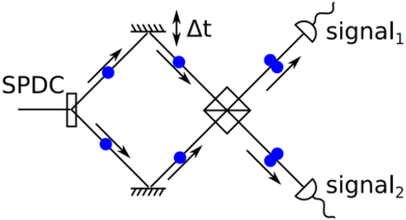


## Joint detection probability

$$P(x_1, x_2) \propto \langle \hat{E}^-(x_1)\hat{E}^-(x_2)\hat{E}^+(x_2)\hat{E}^+(x_1)\rangle$$

$$\hat{E}^+(x_1) = \frac{\epsilon}{\sqrt{2}}(i\hat{a}e^{ik_a x_1} + \hat{b}e^{ik_b x_1})$$

$$\hat{E}^+(x_2) = \frac{\epsilon}{\sqrt{2}}(\hat{a}e^{ik_a x_2} + i\hat{b}e^{ik_b x_2})$$

# Hong-Ou-Mandel effect

Quantum mechanical calculation:

$$\hat{E}^+(x_2)\hat{E}^+(x_1)\left|1\right\rangle_a\left|1\right\rangle_b = \frac{\epsilon^2}{2}\left(e^{i(k_a x_2 + k_b x_1)} - e^{i(k_a x_1 + k_b x_2)}\right)\left|0_a, 0_b\right\rangle$$

$$\left\langle 1\right|_b\left\langle 1\right|_a\hat{E}^-(x_1)\hat{E}^-(x_2) = \frac{\epsilon^2}{2}\left(e^{-i(k_a x_2 + k_b x_1)} - e^{-i(k_a x_1 + k_b x_2)}\right)\left\langle 0_a, 0_b\right|$$

$$P_{a,b} = \frac{\epsilon^4}{2}\left(1 - \cos\big((k_a - k_b)\cdot(x_1 - x_2)\big)\right)$$

$$P_{\text{max}} = \epsilon^4, \quad P_{\text{min}} = 0, \quad \frac{P_{\text{max}} - P_{\text{min}}}{P_{\text{max}} + P_{\text{min}}} = 1$$

But in the classical case:

$$P_{a,b} \propto \langle (I_a + I_b)^2\rangle - 2\langle I_a I_b\rangle \cos\big((k_a - k_b)(x_1 - x_2)\big), \quad \frac{P_{\text{max}} - P_{\text{min}}}{P_{\text{max}} + P_{\text{min}}} < 1$$

# Beam Splitter and Indistinguishable Photons

By injecting **indistinguishable** single photons to each port of the beam splitter, we will have a **pair** of photons in the output ports. The state $|1\rangle_3|1\rangle_4$ does not appear!

$$|\psi\rangle_{\text{in}} = |1\rangle_1|1\rangle_2 = \hat{a}_1^\dagger\hat{a}_2^\dagger|0\rangle_1|0\rangle_2$$

$$\begin{pmatrix} \hat{a}_3 \\ \hat{a}_4 \end{pmatrix} = \frac{1}{\sqrt{2}}\begin{pmatrix} 1 & i \\ i & 1 \end{pmatrix}\begin{pmatrix} \hat{a}_1 \\ \hat{a}_2 \end{pmatrix}$$

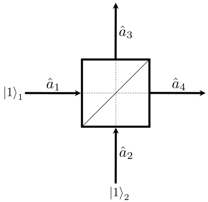


and the fact that the vacuum state is the same before and after BS:

$$\begin{aligned} |\psi\rangle_{\text{out}} &= \frac{1}{2}\left(\hat{a}_3^\dagger + i\hat{a}_4^\dagger\right)\left(i\hat{a}_3^\dagger + \hat{a}_4^\dagger\right)|0\rangle_3|0\rangle_4 \\ &= \frac{1}{2}\left(i\hat{a}^{\dagger 2}_3 + \cancel{\hat{a}^\dagger{}_3\hat{a}^\dagger{}_4} - \cancel{\hat{a}^\dagger{}_4\hat{a}^\dagger{}_3} + i\hat{a}^{\dagger 2}_4\right)|0\rangle_3|0\rangle_4 \\ &= \frac{i}{\sqrt{2}}\left(|2\rangle_3|0\rangle_4 + |0\rangle_3|2\rangle_4\right), \text{ where } [\hat{a}_3, \hat{a}_4] = 0 \end{aligned}$$

# Hong-Ou-Mandel effect with differently polarized photons

## Output state

Consider the case where two single photon states with orthogonal polarization (H, V) enter a 50:50 lossless beamsplitter from port 1 and port 2 individually. The output joint state in port 3 and port 4 can be written as:

$$
\begin{aligned}
|\psi\rangle_{out} &= \hat{a}^\dagger_{1,H}\hat{a}^\dagger_{2,V}|0\rangle_1|0\rangle_2 &(1)\\
&= \frac{1}{2}(\hat{a}^\dagger_{3,H} + i\hat{a}^\dagger_{4,H})(i\hat{a}^\dagger_{3,V} + \hat{a}^\dagger_{4,V})|0\rangle_1|0\rangle_2 &(2)\\
&= \frac{1}{2}(i\hat{a}^\dagger_{3,H}\hat{a}^\dagger_{3,V} + \hat{a}^\dagger_{3,H}\hat{a}^\dagger_{4,V} - \hat{a}^\dagger_{4,H}\hat{a}^\dagger_{3,V} + i\hat{a}^\dagger_{4,H}\hat{a}^\dagger_{4,V})|0\rangle_1|0\rangle_2 &(3)\\
&= \frac{1}{2}(i|1,H\rangle_3|1,V\rangle_3 + |1,H\rangle_3|1,V\rangle_4 - |1,V\rangle_3|1,H\rangle_4 + i|1,H\rangle_4|1,V\rangle_4) &(4)
\end{aligned}
$$

# Indistinguishable Photons From a Single-Photon Device[1]

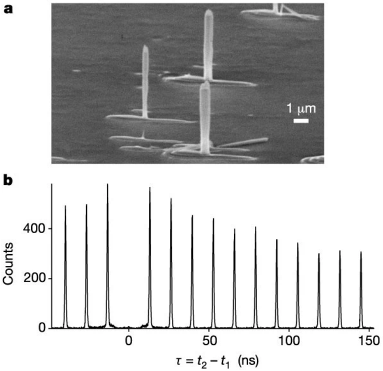


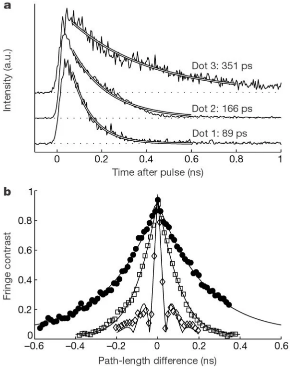


[1] Santori, C., Fattal, D., Vučković, J. et al. Indistinguishable photons from a single-photon device. *Nature* 419, 594–597 (2002)

# Indistinguishable Photons From a Single-Photon Device

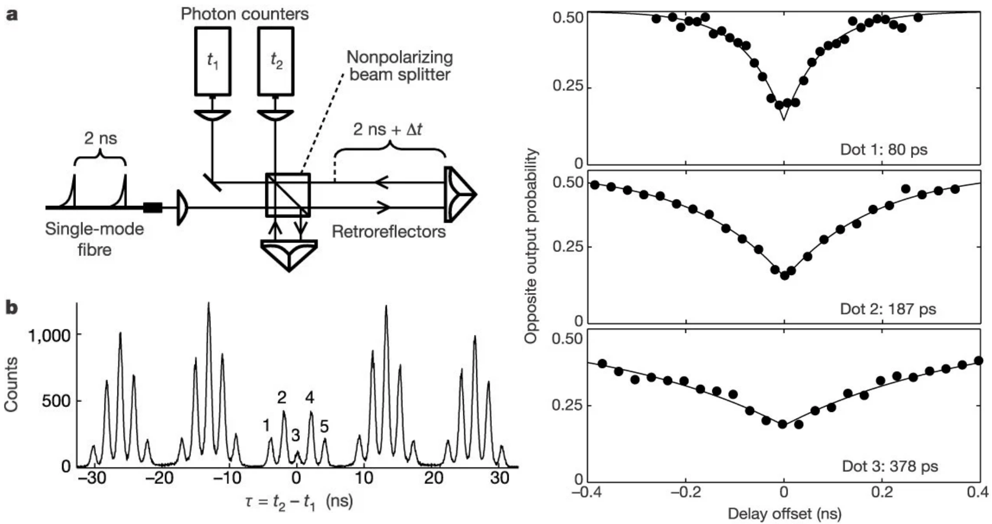

# Wigner Function (E. Wigner, Phys.Rev. 40, 1932)

*JUNE 1, 1932* *PHYSICAL REVIEW* *VOLUME 40*

## On the Quantum Correction For Thermodynamic Equilibrium

By E. Wigner
*Department of Physics, Princeton University*
(Received March 14, 1932)

The probability of a configuration is given in classical theory by the Boltzmann formula $\exp[-V/hT]$ where $V$ is the potential energy of this configuration. For high temperatures this of course also holds in quantum theory. For lower temperatures, however, a correction term has to be introduced, which can be developed into a power series of $h$. The formula is developed for this correction by means of a probability function and the result discussed.



transformations, one can choose any matrix or operator-representation for the $Q$ and $H$. In building the exponential of $H$ one must, of course, take into account the non-commutability of the different parts of $H$.

2

It does not seem to be easy to make explicit calculations with the form (4) of the mean value. One may resort therefore to the following method.

If a wave function $\psi(x_1 \cdots x_n)$ is given one may build the following expression[2]

$$P(x_1, \cdots, x_n; p_1, \cdots, p_n) = \left(\frac{1}{h\pi}\right)^n \int_{-\infty}^{\infty} \cdots \int dy_1 \cdots dy_n \psi(x_1 + y_1 \cdots x_n + y_n)^* \psi(x_1 - y_1 \cdots x_n - y_n) e^{2i(p_1 y_1 + \cdots + p_n y_n)/h} \quad (5)$$

and call it the probability-function of the simultaneous values of $x_1 \cdots x_n$ for the coordinates and $p_1 \cdots p_n$ for the momenta. In (5), as throughout this paper, $h$ is the Planck constant divided by $2\pi$ and the integration with respect to the $y$ has to be carried out from $-\infty$ to $\infty$. Expression (5) is real, but not everywhere positive. It has the property, that it gives, when integrated with respect to the $p$, the correct probabilities $|\psi(x_1 \cdots x_n)|^2$ for the different values of the coordinates and also it gives, when integrated with respect to the $x$, the correct quantum mechanical probabilities

$$\left| \int_{-\infty}^{\infty} \cdots \int \psi(x_1 \cdots x_n) e^{-i(p_1 x_1 + \cdots + p_n x_n)/h} dx_1 \cdots dx_n \right|^2$$

for the momenta $p_1, \cdots, p_n$. The first fact follows simply from the theorem about the Fourier integral and one gets the second by introducing $x_k + y_k = u_k$; $x_k - y_k = v_k$ into (5).

# Wigner Function[2]

## Wigner function, the phase-space quasi-probability density

$$W_{\hat{\rho}}(q,p) = \frac{1}{2\pi}\int_{-\infty}^{\infty} \left\langle q + \frac{1}{2}q' \middle| \hat{\rho} \middle| q - \frac{1}{2}q' \right\rangle e^{-ipq'} dq'$$

This function uniquely defines the state and directly relates to the quadrature histograms measured experimentally via

$$\mathrm{Pr}(q_\theta, \theta) = \int_{-\infty}^{\infty} W_{\mathrm{det}}(q_\theta \cos\theta - p_\theta \sin\theta, q_\theta \sin\theta + p_\theta \cos\theta) dp_\theta.$$

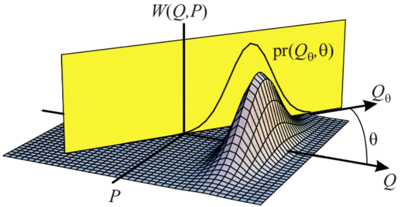


The experimentally measured probability density $\mathrm{Pr}(q_\theta, \theta)$ is the integral projection of the Wigner function $W_{\hat{\rho}}(q,p)$ onto a vertical plane defined by the phase of the local oscillator.

[2] Lvovsky, Alexander I., and Michael G. Raymer. "Continuous-variable optical quantum-state tomography." *Reviews of Modern Physics* 81.1 (2009): 299.

# Examples for calculation of Wigner function

## Vacuum state

The wavefunction of harmonic oscillator ground state is (assume $\hbar = 1$)

$$\psi_0(x) = (\frac{1}{\pi})^{1/4} e^{-x^2/2}$$

The corresponding Wigner function is calculated as

$$W(x,p) = \frac{1}{2\pi} \int_{-\infty}^{\infty} \langle x + y/2 | \psi_0 \rangle \langle \psi_0 | x - y/2 \rangle e^{-ipy} dy \tag{5}$$

$$= \frac{1}{2\pi} \int_{-\infty}^{\infty} \psi_0^*(x + y/2) \psi_0(x - y/2) e^{-ipy} dy \tag{6}$$

$$= \frac{1}{2\pi^{3/2}} \int_{-\infty}^{\infty} e^{-\frac{(x+y/2)^2}{2} - \frac{(x-y/2)^2}{2} - ipy} dy \tag{7}$$

$$= \frac{1}{\pi} e^{-x^2 - p^2} \tag{8}$$

# Wigner Function

## Vacuum state

Transform back to phase-space representation using $x = \frac{\alpha+\alpha^*}{\sqrt{2}}$ and $p = \frac{\alpha-\alpha^*}{i\sqrt{2}}$

$$W(\alpha,\alpha^*) = \frac{2}{\pi}e^{-2|\alpha|^2}$$

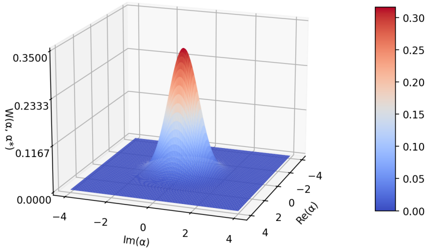


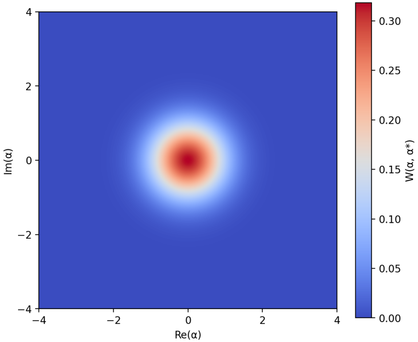

# Examples for calculation of Wigner function

## Fock state (n=1)

The wavefunction of harmonic oscillator first excited state is (assume $\hbar = 1$)

$$\psi_1(x) = \frac{\sqrt{2}x}{\pi^{1/4}} e^{-x^2/2}$$

The corresponding Wigner function is calculated as

$$W(x,p) = \frac{1}{2\pi} \int_{-\infty}^{\infty} \langle x + y/2 | \psi_1 \rangle \langle \psi_1 | x - y/2 \rangle e^{-ipy} dy \tag{9}$$

$$= \frac{1}{2\pi} \int_{-\infty}^{\infty} \psi_1^*(x + y/2) \psi_1(x - y/2) e^{-ipy} dy \tag{10}$$

$$= \frac{1}{\pi^{3/2}} \int_{-\infty}^{\infty} (x + y/2)(x - y/2) e^{-\frac{(x+y/2)^2}{2} - \frac{(x-y/2)^2}{2} - ipy} dy \tag{11}$$

$$= \frac{1}{\pi} (2x^2 + 2p^2 - 1) e^{-x^2 - p^2} \tag{12}$$

# Examples for calculation of Wigner function

## Fock state (n=1)

Transform back to phase-space representation using $x = \frac{\alpha+\alpha^*}{\sqrt{2}}$ and $p = \frac{\alpha-\alpha^*}{i\sqrt{2}}$

$$W(\alpha,\alpha^*) = \frac{2}{\pi}(4|\alpha|^2 - 1)e^{-2|\alpha|^2}$$

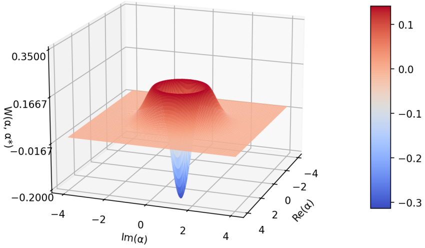


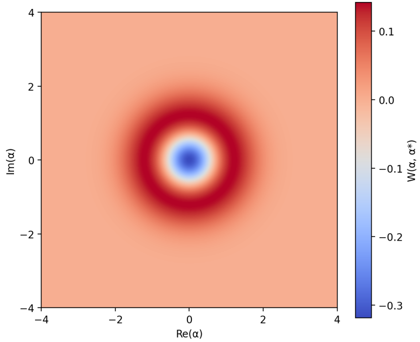

# Other examples of Wigner Function

## Coherent state

$$\alpha = \frac{1}{2}(X_1 + iX_2), \qquad X_i = \langle \hat{x}_i \rangle$$

$$\langle (\Delta \hat{x}_1)^2 \rangle = \langle (\Delta \hat{x}_2)^2 \rangle = 1$$

$$W(x_1', x_2') = \frac{2}{\pi} e^{-\frac{1}{2}(x_1'^2 + x_2'^2)}, \qquad x_i' = x_i - X_i$$

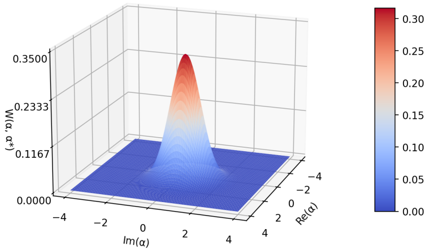


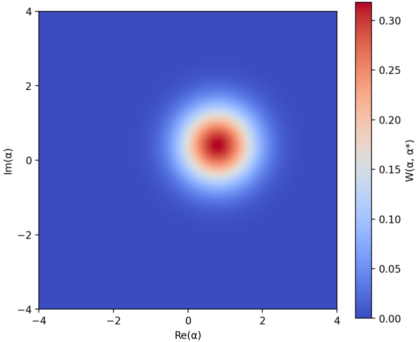

# Other examples of Wigner Function

## Squeezed state

$$W(x_1', x_2') = \frac{2}{\pi} e^{-\frac{1}{2}(x_1'^2 e^{-2r} + x_2'^2 e^{+2r})}$$

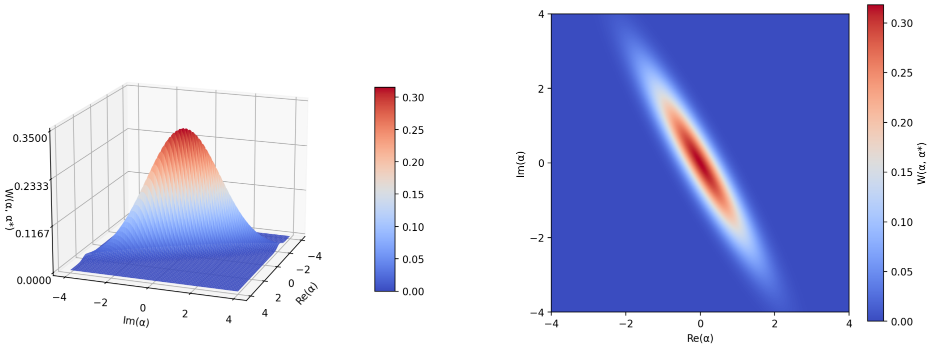

# Influence of a beamsplitter splitting ratio on Wigner function measurement

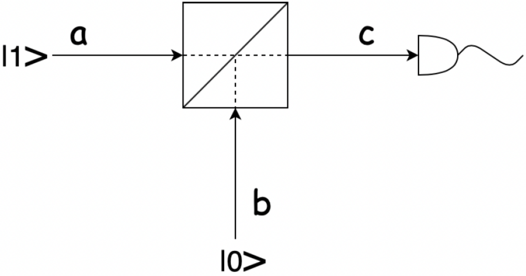


$$\hat{c} = \sqrt{\eta}\hat{a} + i\sqrt{1-\eta}\hat{b}$$

If we measure the Wigner function at port c, with $\eta$ larger than 0.5, the negativity of the Wigner function is observable.

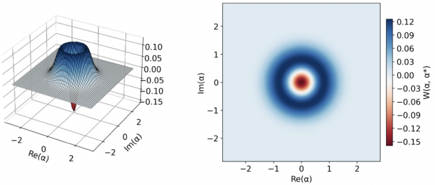


Figure: $\eta = 0.75$

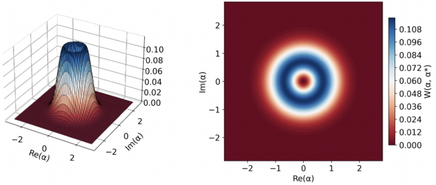


Figure: $\eta = 0.5$

# Wigner function

## Symmetric Characteristic Function

$$\chi_s \equiv \mathbf{Tr}[\rho e^{\beta a^\dagger - \beta^* a}] \equiv \mathbf{Tr}[\rho D(\beta)]$$

$$W(\alpha, \alpha^*) \equiv \frac{1}{\pi^2} \int \chi_s(\beta, \beta^*) e^{-\beta\alpha^*} e^{\beta^*\alpha} \mathrm{d}^2\beta$$

$$\left\langle \frac{a^\dagger a + a a^\dagger}{2} \right\rangle = \int W(\alpha)\, \alpha^* \alpha \, \mathrm{d}^2\alpha$$

## Calculation of Wigner Function

If $\rho = |\phi\rangle \langle\phi|$, then

$$\boxed{W_\phi(\alpha, \alpha^*) = \frac{1}{\pi^2} \int \mathrm{d}^2 z \, e^{\beta^*\alpha - \beta\alpha^*} \, \langle\phi| \, D(\beta) \, |\phi\rangle}$$

# Quantum State Tomography

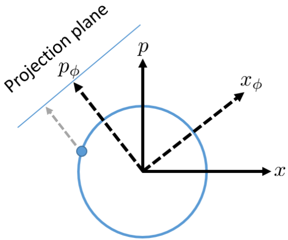


$W(p,q)$ is a joint probability function for the $\hat{p}$ and $\hat{q}$ operators:

## Marginals

$$\Pr(q_\phi) = \left\langle q_\phi \middle| \hat{\rho} \middle| q_\phi \right\rangle = \int_{-\infty}^{\infty} W(p,q) dp_\phi, \text{ where}$$

$$\hat{q}_\phi = \hat{q}\cos(\phi) + \hat{p}\sin(\phi), \quad \hat{p}_\phi = -\hat{q}\sin(\phi) + \hat{p}\cos(\phi)$$

# Quantum State Tomography

## Motivation

To reconstruct a quantum state of light, we cannot directly measure $\rho_{nn}$ with a photo-detector but we can measure $\mathrm{Pr}(X_\theta)$ and reconstruct the full Wigner function. For rotationally symmetric states e.g. Fock states the reconstruction becomes Abel transform[3]:

$$X_\theta = \langle X_\theta | \rho | X_\theta \rangle = \langle X | U_\theta^\dagger \rho U_\theta | X \rangle$$

$$\mathrm{Pr}(X_\theta) = \int_{-\infty}^{\infty} W(p_\theta, q_\theta) dp_\theta$$

$$W(r) = -\frac{1}{\pi} \int_r^\infty \frac{d\mathrm{Pr}(q_\phi)}{dq_\phi} (q_\phi^2 - r^2)^{-1/2} dq_\phi.$$

[3] Vogel, W., Welsch, D.G. "Quantum Optics" (2001). Chapter 7

# Wigner Function and Parity Operator

## Alternative expression for the Wigner function[4]

$$W(r,p) = \frac{1}{h^2}\int dk \int ds e^{-i\frac{kr+sp}{h}} \langle\psi| e^{-i\frac{k\hat{R}+s\hat{P}}{h}} |\psi\rangle = \frac{2}{h}\langle\psi|\hat{\Pi}_{rp}|\psi\rangle$$

Where $\hat{\Pi}_{rp} = \hat{D}(r,p)\hat{\Pi}\hat{D}^{-1}(r,p)$ is a displaced parity operator $\hat{\Pi}$, which acts as follows

$$\hat{\Pi}\hat{R}\hat{\Pi} = -\hat{R}$$
$$\hat{\Pi}\hat{P}\hat{\Pi} = -\hat{P}$$

**Wigner function as the expectation value of a parity operator**

Antoine Royer
*Centre de Recherches Mathématiques, Université de Montréal, Montréal H3C 3J7, Canada*
(Received 30 August 1976)

It is pointed out that the Wigner function $f(r,p)$ is $2/h$ times the expectation value of the parity operator that performs reflections about the phase-space point $r, p$. Thus $f(r,p)$ is proportional to the overlap of the wave function $\psi$ with its mirror image about $r, p$; this is clearly a measure of how much $\psi$ is *centered* about $r, p$, and the Wigner distribution function now appears physically more meaningful and natural than it did previously.

[4] Moyal JE. Quantum mechanics as a statistical theory. Mathematical Proceedings of the Cambridge Philosophical Society. 1949;45(1):99-124. doi:10.1017/S0305004100000487

# State Reconstruction

## Inverse Radon transformation

$$W_{\text{det}}(q,p) = \frac{1}{2\pi^2}\int_0^{\pi}\int_{-\infty}^{\infty}\text{Pr}(q_\theta,\theta)\times K(q\cos\theta + p\sin\theta - q_\theta)dq_\theta d\theta$$

with the integration kernel $K(x) = \frac{1}{2}\int_{-\infty}^{\infty}|\xi|e^{i\xi x}d\xi$. The density matrix can then be reconstructed using the pattern function method.

## Maximum likelihood reconstruction

$$L = \Pi_i \text{Pr}_{\hat{\rho}}(q_i, \theta_i)$$

is the likelihood function given the measured data set $\{(q_i, \theta_i)\}$ where $\hat{\rho}$ is the density matrix to be optimized.

# State Reconstruction

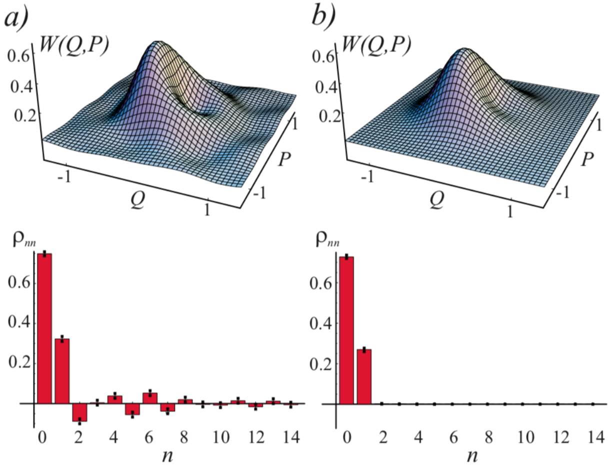


Quantum optical state estimation from a set of 14152 experimental homodyne measurements by means of (a) the inverse Radon tranformation and the pattern-function method and (b) the likelihood maximization algorithm. The Wigner function and the diagonal elements of the reconstructed density matrix are shown.

The original Radon transformation paper in German.

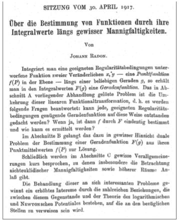

SITZUNG VOM 30. APRIL 1917.

**Über die Bestimmung von Funktionen durch ihre Integralwerte längs gewisser Mannigfaltigkeiten.**

Von

Johann Radon.

Integriert man eine geeigneten Regularitätsbedingungen unterworfene Funktion zweier Veränderlichen $x, y$ — eine *Punktfunktion* $f(P)$ in der Ebene — längs einer beliebigen Geraden $g$, so erhält man in den Integralwerten $F(g)$ eine *Geradenfunktion*. Das in Abschnitt A vorliegender Abhandlung gelöste Problem ist die Umkehrung dieser linearen Funktionaltransformation, d. h. es werden folgende Fragen beantwortet: kann jede, geeigneten Regularitätsbedingungen genügende Geradenfunktion auf diese Weise entstanden gedacht werden? Wenn ja, ist dann $f$ durch $F$ eindeutig bestimmt und wie kann es ermittelt werden?

Im Abschnitte B gelangt das dazu in gewisser Hinsicht duale Problem der Bestimmung einer Geradenfunktion $F(g)$ aus ihren Punktmittelwerten $f(P)$ zur Lösung.

Schließlich werden im Abschnitte C gewisse Verallgemeinerungen kurz besprochen, zu denen insbesondere die Betrachtung nichteuklidischer Mannigfaltigkeiten sowie höherer Räume Anlaß gibt.

Die Behandlung dieser an sich interessanten Probleme gewinnt ein erhöhtes Interesse durch die zahlreichen Beziehungen, die zwischen diesem Gegenstande und der Theorie des logarithmischen und Newtonschen Potentiales bestehen, auf die an den bezüglichen Stellen zu verweisen sein wird.

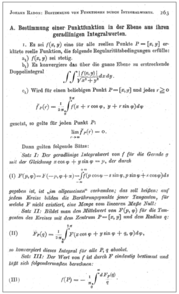

Johann Radon: Bestimmung von Funktionen durch Integralwerte. 263

**A. Bestimmung einer Punktfunktion in der Ebene aus ihren geradlinigen Integralwerten.**

1. Es sei $f(x, y)$ eine für alle reellen Punkte $P = [x, y]$ erklärte reelle Funktion, die folgende Regularitätsbedingungen erfülle:

$a_1$) $f(x, y)$ sei stetig.

$b_1$) Es konvergiere das über die ganze Ebene zu erstreckende Doppelintegral

$$\iint \frac{|f(x,y)|}{\sqrt{x^2+y^2}}\,dx\,dy.$$

$c_1$) Wird für einen beliebigen Punkt $P = [x, y]$ und jedes $r \geqq 0$

$$\bar{f}_P(r) = \frac{1}{2\pi}\int_0^{2\pi} f(x + r\cos\varphi,\ y + r\sin\varphi)\,d\varphi$$

gesetzt, so gelte für jeden Punkt $P$:

$$\lim_{r\to\infty} \bar{f}_P(r) = 0.$$

Dann gelten folgende Sätze:

*Satz I: Der geradlinige Integralwert von $f$ für die Gerade $g$ mit der Gleichung $x\cos\varphi + y\sin\varphi = p$, der durch*

$$\text{(I)}\quad F(p,\varphi) = F(-p,\varphi+\pi) = \int_{-\infty}^{+\infty} f(p\cos\varphi - s\sin\varphi,\ p\sin\varphi + s\cos\varphi)\,ds$$

*gegeben ist, ist „im allgemeinen" vorhanden; das soll heißen: auf jedem Kreise bilden die Berührungspunkte jener Tangenten, für welche $F$ nicht existiert, eine Menge vom linearen Maße Null:*

*Satz II: Bildet man den Mittelwert von $F(p, \varphi)$ für die Tangenten des Kreises mit dem Zentrum $P = [x, y]$ und dem Radius $q$:*

$$\text{(II)}\qquad \bar{F}_P(q) = \frac{1}{2\pi}\int_0^{2\pi} F(x\cos\varphi + y\sin\varphi + q,\ \varphi)\,d\varphi,$$

*so konvergiert dieses Integral für alle $P$, $q$ absolut.*

*Satz III: Der Wert von $f$ ist durch $F$ eindeutig bestimmt und läßt sich folgendermaßen berechnen:*

$$\text{(III)}\qquad f(P) = -\frac{1}{\pi}\int_0^{\infty} \frac{d\bar{F}_P(q)}{q}.$$

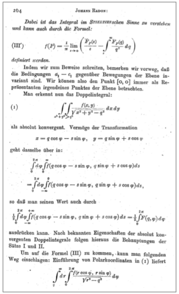

264 Johann Radon:

*Dabei ist das Integral im Stieltjesschen Sinne zu verstehen und kann auch durch die Formel:*

$$\text{(III')}\qquad f(P) = \frac{1}{\pi}\lim_{\varepsilon\to 0}\left(\frac{\bar{F}_P(\varepsilon)}{\varepsilon} - \int_\varepsilon^{\infty} \frac{\bar{F}_P(q)}{q^2}\,dq\right)$$

*definiert werden.*

Indem wir zum Beweise schreiten, bemerken wir vorweg, daß die Bedingungen $a_1 - c_1$ gegenüber Bewegungen der Ebene invariant sind. Wir können also den Punkt $[0, 0]$ immer als Repräsentanten irgendeines Punktes der Ebene betrachten.

Man erkennt nun das Doppelintegral:

$$\text{(1)}\qquad \iint_{x^2+y^2>q^2} \frac{f(x,y)}{\sqrt{x^2+y^2-q^2}}\,dx\,dy$$

als absolut konvergent. Vermöge der Transformation

$$x = q\cos\varphi - s\sin\varphi, \quad y = q\sin\varphi + s\cos\varphi$$

geht dasselbe über in:

$$\int_0^{2\pi} d\varphi \int_0^{\infty} f(q\cos\varphi - s\sin\varphi,\ q\sin\varphi + s\cos\varphi)\,ds$$

$$= \int_0^{2\pi} d\varphi \int_{-\infty}^{0} f(q\cos\varphi - s\sin\varphi,\ q\sin\varphi + s\cos\varphi)\,ds,$$

so daß man seinen Wert auch durch

$$\frac{1}{2}\int_0^{2\pi} d\varphi \int_{-\infty}^{+\infty} f(q\cos\varphi - s\sin\varphi,\ q\sin\varphi + s\cos\varphi)\,ds = \frac{1}{2}\int_0^{2\pi} F(q,\varphi)\,d\varphi$$

ausdrücken kann. Nach bekannten Eigenschaften der absolut konvergenten Doppelintegrale folgen hieraus die Behauptungen der Sätze I und II.

Um auf die Formel (III) zu kommen, kann man folgenden Weg einschlagen: Einführung von Polarkoordinaten in (1) liefert

$$\int_q^{\infty} dr \int_0^{2\pi} \frac{f(r\cos\varphi,\ r\sin\varphi)}{\sqrt{r^2-q^2}}\,d\varphi$$

# State Reconstruction Experiment[5]

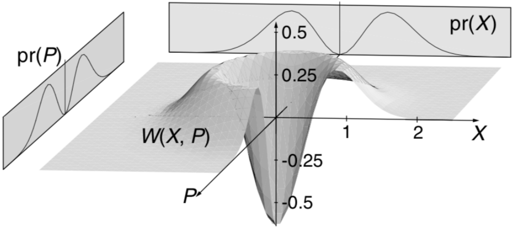


FIG. 1. Theoretical phase space quasiprobability density (Wigner function) of the single-photon state $|1\rangle$: $W(X,P) = \frac{2}{\pi}[4(X^2+P^2)-1]e^{-2(X^2+P^2)}$. $\hat{X} = (\hat{a}+\hat{a}^\dagger)/\sqrt{2}$ and $\hat{P} = (\hat{a}-\hat{a}^\dagger)/\sqrt{2}i$ are normalized noncommuting electric field quadrature observables. Single-quadrature probability densities (*marginal distributions*) are also displayed.

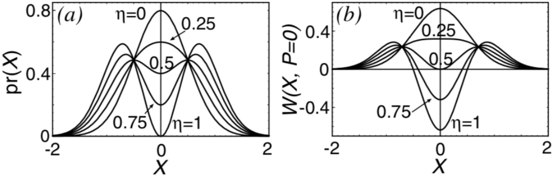


FIG. 3. Effect of the nonperfect measurement efficiency $\eta$ on the marginal distribution (a) and the reconstructed WF (b). For the WF, cross sections by the plane $P = 0$ are shown. Negative values require $\eta > 0.5$.

[5] Lvovsky, Alexander I., et al. "Quantum state reconstruction of the single-photon Fock state." *Physical Review Letters* 87.5 (2001): 050402.

# State Reconstruction Experiment

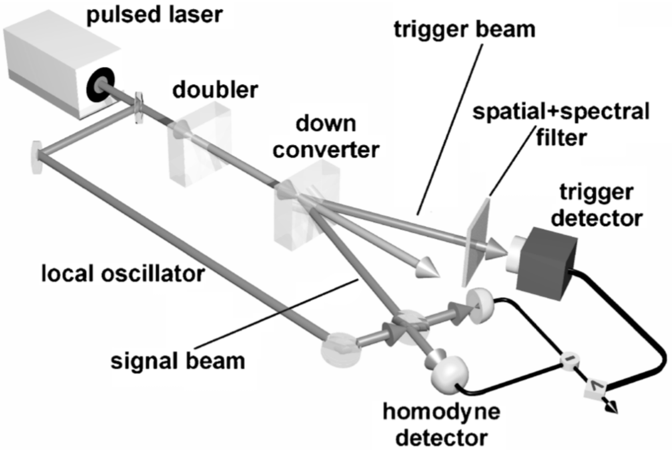


FIG. 2. Simplified scheme of the experimental setup.

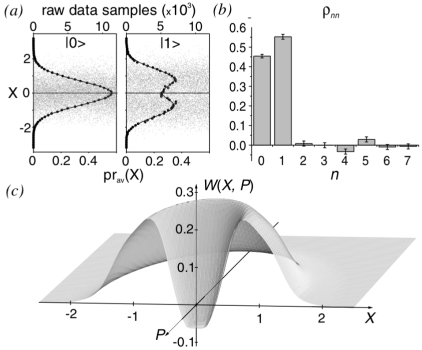


FIG. 4. Experimental results: (a) raw quantum noise data for the vacuum (left) and Fock (right) states along with their histograms corresponding to the phase-randomized marginal distributions; (b) diagonal elements of the density matrix of the state measured; (c) reconstructed WF which is negative near the origin point. The measurement efficiency is 55%.

# Two Mode Squeezed Vacuum State

$$\hat{S}_{\text{two-mode}} = e^{r\hat{a}^\dagger\hat{b}^\dagger - r\hat{a}\hat{b}}$$

$$|\Psi\rangle = \frac{1}{\cosh(r)}\sum_{n=0}^{\infty}(\tanh(r))^n\,|n,n\rangle$$

**Wave-function associated with the state:**

$$\langle Q_1, Q_2|\Psi\rangle = \frac{1}{\sqrt{\pi}}\exp\left(-\frac{1}{4}e^{2r}(Q_1 - Q_2)^2 - \frac{1}{4}e^{-2r}(Q_1 + Q_2)^2\right)$$

$$\langle P_1, P_2|\Psi\rangle = \frac{1}{\sqrt{\pi}}\exp\left(-\frac{1}{4}e^{2r}(P_1 - P_2)^2 - \frac{1}{4}e^{-2r}(P_1 + P_2)^2\right)$$

# Two mode squeezed vacuum state

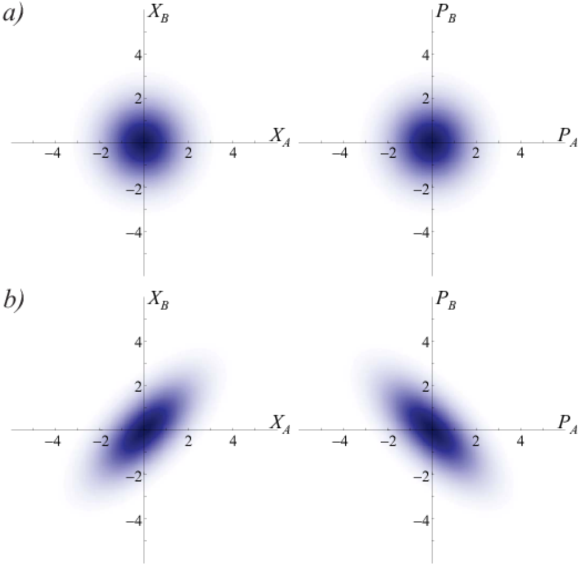

# Covariance matrix

Since squeezed states are Gaussian states (with Gaussian statistics), 4 numbers characterize their full state: $\{V_{xx}, V_{xy}, V_{yx}, V_{yy}\}$

## Definition of covariance matrix

$$V_{xy} = \frac{\langle \hat{X}\hat{Y} + \hat{Y}\hat{X} \rangle - 2\langle \hat{X} \rangle \langle \hat{Y} \rangle}{2\Delta \hat{X}^2_{vac}}$$

From covariance matrix one can determine the amount of entanglement ("Logarithmic negativity" : The logarithmic negativity is an entanglement measure which is easily computable and an upper bound to the distillable entanglement).

# Unconditional Quantum Teleportation

**A. Furusawa, J. L. Sørensen, S. L. Braunstein, C. A. Fuchs, H. J. Kimble,* E. S. Polzik**

Quantum teleportation of optical coherent states was demonstrated experimentally using squeezed-state entanglement. The quantum nature of the achieved teleportation was verified by the experimentally determined fidelity $F^{exp} = 0.58 \pm 0.02$, which describes the match between input and output states. A fidelity greater than 0.5 is not possible for coherent states without the use of entanglement. This is the first realization of unconditional quantum teleportation where every state entering the device is actually teleported.

# Unconditional Quantum Teleportation

**Fig. 1.** Schematic of the experimental apparatus for teleportation of an unknown quantum state $|v_{in}\rangle$ from Alice's sending station to Bob's receiving terminal by way of the classical information $(i_x, i_p)$ sent from Alice to Bob and the shared entanglement of the EPR beams (1, 2).

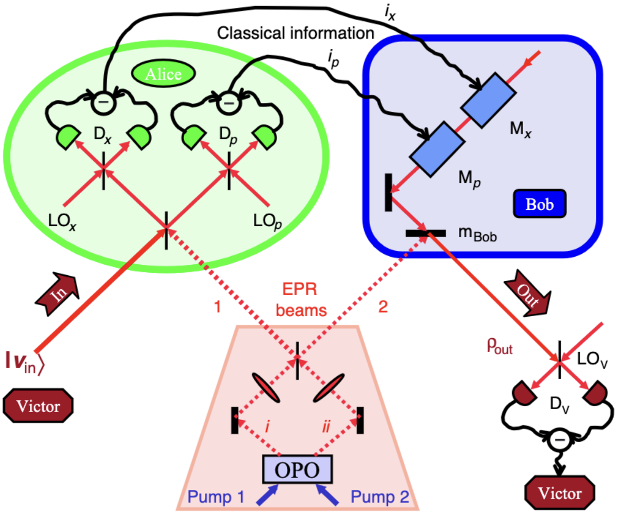

# Unconditional Quantum Teleportation

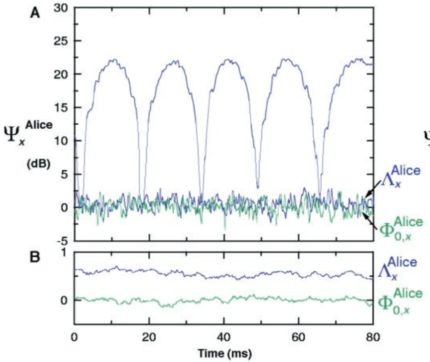


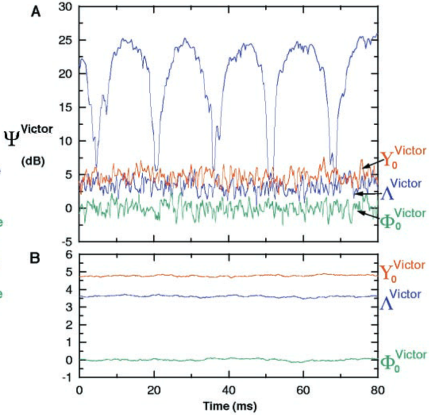


**Fig. 2 (left).** (**A**) Spectral density of photocurrent fluctuations $\Psi_x^{\text{Alice}}(\Omega)$ recorded by Alice's balanced homodyne detector $D_x$ as a function of time with the phase $\phi_{\text{in}}$ of the coherent-state input linearly swept. For the case of a vacuum-state input $v_{\text{in}} = 0$ and with no EPR beams present, the vacuum-state level $\Phi_{0,x}^{\text{Alice}}(\Omega)$ results, whereas with $v_{\text{in}} = 0$ and EPR beam 1 distributed to Alice, excess noise at the level $\Lambda_x^{\text{Alice}}(\Omega)$ is recorded. (**B**) Expanded view for $v_{\text{in}} = 0$, now with a 10-trace average. Acquisition parameters: radio frequency (rf) $\Omega/2\pi = 2.9$ MHz, rf bandwidth $\Delta\Omega/2\pi = 30$ kHz, video bandwidth = 1 kHz (A) and 30 Hz (B). **Fig. 3 (right).** (**A**) Spectral density of photocurrent fluctuations $\Psi^{\text{Victor}}(\Omega)$ recorded by Victor's balanced homodyne detector $D_V$ as afunction of time with the phase $\phi_{\text{in}}$ of the coherent-state input linearly swept and with the gain $g \approx 1$. For the case of a vacuum-state input $v_{\text{in}} = 0$ and with no EPR beams present, the excess noise level $\Upsilon_0^{\text{Victor}}(\Omega)$ results, whereas with $v_{\text{in}} = 0$ and EPR beams {1, 2} distributed to Alice and Bob, the level of fluctuations is reduced to $\Lambda^{\text{Victor}}(\Omega)$. The vacuum-state level for $D_V$ is given by $\Phi_0^{\text{Victor}}$. (**B**) Expanded view for $v_{\text{in}} = 0$, now with a 10-trace average. Acquisition parameters are as in Fig. 2.

# Unconditional Quantum Teleportation

our actual experiment, we calculate $F$ for the case of a finite degree of EPR correlation and in the presence of non-unit efficiencies, which for a coherent-state input $|v_{\mathrm{in}}\rangle$ becomes

$$F = 2/\sigma_Q \exp[-2|v_{\mathrm{in}}|^2(1-g)^2/\sigma_Q] \quad (2)$$

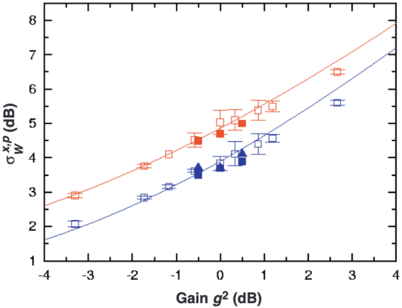


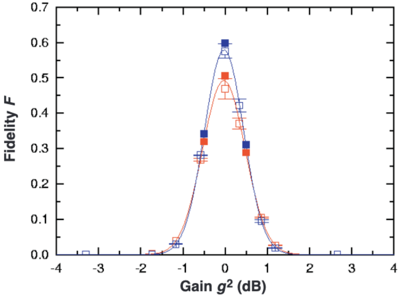


**Fig. 4 (left).** Variance $\sigma_W^{x,p}$ of the teleported field measured by Victor as a function of the gain $g$ used by Bob for the phase-space displacement of the EPR beam 2. Shown are data obtained both with the quantum-correlated EPR beams present (blue) and with vacuum-state inputs (red) for beams {1, 2}. Open and filled symbols represent results of two different experiments. The theoretical results from Eq. 2 (curves) are also shown for the two cases of quantum and classical teleportation. **Fig. 5 (right).** Fidelity $F$ inferred from measurements of the input amplitude $v_{\mathrm{in}}$ and of the quantities $v_{\mathrm{out}}$ and $\sigma_Q^{x,p}$ for the teleported output field. Data for the cases of classical (red) and quantum (blue) teleportation are shown, as are the theoretical results from Eq. 1 (curves). See text for explanations of filled and open symbols. $F > 0.5$ demonstrates the nonclassical nature of the protocol.

# Paper for this week

VOLUME 87, NUMBER 5 PHYSICAL REVIEW LETTERS 30 JULY 2001

## Quantum State Reconstruction of the Single-Photon Fock State

A. I. Lvovsky,* H. Hansen, T. Aichele, O. Benson, J. Mlynek,† and S. Schiller‡
*Fachbereich Physik, Universität Konstanz, D-78457 Konstanz, Germany*
(Received 14 March 2001; published 11 July 2001)

We have reconstructed the quantum state of optical pulses containing single photons using the method of phase-randomized pulsed optical homodyne tomography. The single-photon Fock state $|1\rangle$ was prepared using conditional measurements on photon pairs born in the process of parametric down-conversion. A probability distribution of the phase-averaged electric field amplitudes with a strongly non-Gaussian shape is obtained with the total detection efficiency of $(55 \pm 1)\%$. The angle-averaged Wigner function reconstructed from this distribution shows a strong dip reaching classically impossible negative values around the origin of the phase space.

DOI: 10.1103/PhysRevLett.87.050402 PACS numbers: 03.65.Wj, 42.50.Dv

# Paper for this week

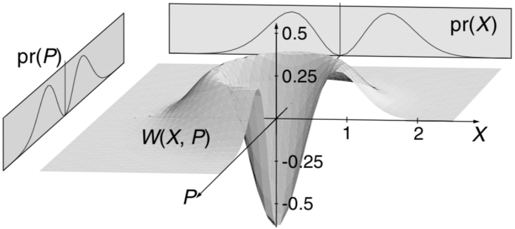


FIG. 1. Theoretical phase space quasiprobability density (Wigner function) of the single-photon state $|1\rangle$: $W(X,P) = \frac{2}{\pi}[4(X^2 + P^2) - 1]e^{-2(X^2+P^2)}$. $\hat{X} = (\hat{a} + \hat{a}^\dagger)/\sqrt{2}$ and $\hat{P} = (\hat{a} - \hat{a}^\dagger)/\sqrt{2}i$ are normalized noncommuting electric field quadrature observables. Single-quadrature probability densities (*marginal distributions*) are also displayed.

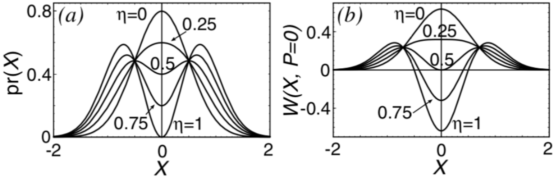


FIG. 3. Effect of the nonperfect measurement efficiency $\eta$ on the marginal distribution (a) and the reconstructed WF (b). For the WF, cross sections by the plane $P = 0$ are shown. Negative values require $\eta > 0.5$.

# Paper for this week

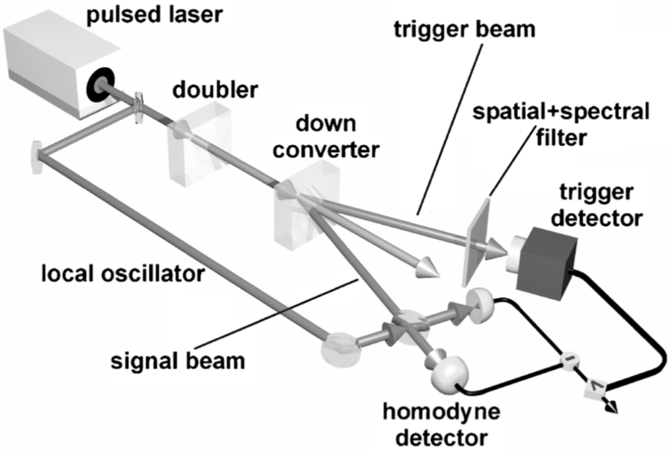


FIG. 2. Simplified scheme of the experimental setup.

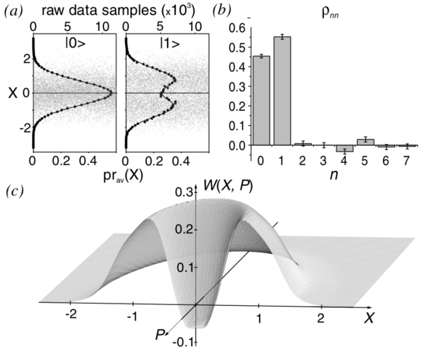


FIG. 4. Experimental results: (a) raw quantum noise data for the vacuum (left) and Fock (right) states along with their histograms corresponding to the phase-randomized marginal distributions; (b) diagonal elements of the density matrix of the state measured; (c) reconstructed WF which is negative near the origin point. The measurement efficiency is 55%.

# Paper for next week

PHYSICAL REVIEW A **76**, 042319 (2007)

## Charge-insensitive qubit design derived from the Cooper pair box

Jens Koch,[1] Terri M. Yu,[1] Jay Gambetta,[1] A. A. Houck,[1] D. I. Schuster,[1] J. Majer,[1] Alexandre Blais,[2] M. H. Devoret,[1] S. M. Girvin,[1] and R. J. Schoelkopf[1]

[1]*Departments of Physics and Applied Physics, Yale University, New Haven, Connecticut 06520, USA*

[2]*Département de Physique et Regroupement Québécois sur les Matériaux de Pointe, Université de Sherbrooke, Sherbrooke, Québec, Canada J1K 2R1*

(Received 22 May 2007; published 12 October 2007)

Short dephasing times pose one of the main challenges in realizing a quantum computer. Different approaches have been devised to cure this problem for superconducting qubits, a prime example being the operation of such devices at optimal working points, so-called "sweet spots." This latter approach led to significant improvement of $T_2$ times in Cooper pair box qubits [D. Vion *et al.*, Science **296**, 886 (2002)]. Here, we introduce a new type of superconducting qubit called the "transmon." Unlike the charge qubit, the transmon is designed to operate in a regime of significantly increased ratio of Josephson energy and charging energy $E_J/E_C$. The transmon benefits from the fact that its charge dispersion decreases exponentially with $E_J/E_C$, while its loss in anharmonicity is described by a weak power law. As a result, we predict a drastic reduction in sensitivity to charge noise relative to the Cooper pair box and an increase in the qubit-photon coupling, while maintaining sufficient anharmonicity for selective qubit control. Our detailed analysis of the full system shows that this gain is not compromised by increased noise in other known channels.

DOI: 10.1103/PhysRevA.76.042319 PACS number(s): 03.67.Lx, 74.50.+r, 32.80.−t

# Questions for this week's paper

- What's the expression for Wigner function the authors use?
- What measurement data is taken and how is it used to reconstruct the Wigner function?
- How does measurement efficiency impact the result?
- How does signal-LO mode-matching influence efficiency in homodyne detection?
- Why a single laser is used for both the local-oscillator and the signal?
- Why do they use a doubler and down-converter as a source of single photons?
- How does the spatial-temporal pulse shape of single photon match LO?
- How is the density matrix reconstructed? What is the physical meaning of the off-diagonal values of the density-operator?